Received: 14 October 2024 | Accepted: 30 January 2025

DOI: 10.1097/HC9.0000000000000684

ORIGINAL ARTICLE

OPEN

The ferroptosis mediator ACSL4 fails to prevent disease progression in mouse models of MASLD

Carolin Angendohr[1] | Christiane Koppe[1] | Diran Herebian[2] | Anne T. Schneider[1] | Leonie Keysberg[1] | Michael T. Singer[1] | Julian Gilljam[1] | Matthias A. Dille[1] | Johannes G. Bode[1] | Sebastian Doll[3] | Marcus Conrad[3] | Mihael Vucur[1] | Tom Luedde[1]

[1]Department of Gastroenterology, Hepatology and Infectious Diseases, Faculty of Medicine & Düsseldorf University Hospital, Heinrich-Heine-University, Düsseldorf, Germany

[2]Department of General Pediatrics, Neonatology and Pediatric Cardiology, Medical Faculty and University Hospital, Heinrich Heine University, Düsseldorf, Germany

[3]Institute of Developmental Genetics, Helmholtz Zentrum München, Neuherberg, Germany

Correspondence
Tom Luedde, Department of Gastroenterology, Hepatology and Infectious Diseases, University-Hospital Düsseldorf, Heinrich-Heine-University Düsseldorf, Moorenstrasse 5, Düsseldorf 40225, Germany.
Email: luedde@hhu.de

Abstract

Background: Metabolic dysfunction–associated steatotic liver disease (MASLD) is an increasingly prevalent condition and a major risk factor for chronic liver damage, potentially leading to steatohepatitis and HCC. It is already known that patients with MASLD show increased systemic and hepatic iron concentrations as well as perturbed lipid metabolism, suggesting the involvement of ferroptosis in the development and progression of MASLD. Consequently, inhibition of ferroptosis represents a potential therapeutic option for patients with MASLD.

Methods: We investigated whether liver parenchymal cell–specific deletion (LPC-KO) of the pro-ferroptotic gene acyl-CoA synthetase long-chain family member 4 ($ACSL4^{LPC\text{-}KO}$) reduces MASLD onset and progression in mice. $ACSL4^{LPC\text{-}KO}$ and wild-type littermates were fed a choline-deficient high-fat diet (CD-HFD) or a Western diet for 20 weeks (CD-HFD and Western diet) or 40 weeks (CD-HFD only) to monitor MASLD progression and metabolic syndrome development.

Results: In contrast to the recently published studies by Duan et al, our results show no significant differences between $ACSL4^{LPC\text{-}KO}$ and wild-type mice with regard to the development of MASLD or the progression of metabolic syndrome. Furthermore, no differences were observed in metabolic parameters (ie, weight gain, glucose tolerance test, hepatic steatosis) or MASLD-associated inflammatory response.

Abbreviations: ACSL4, acyl-CoA synthetase long-chain family member 4; $ACSL4^{LPC\text{-}KO}$, liver parenchymal cell-specific deletion of pro-ferroptotic gene acyl-CoA synthetase long-chain family member 4; CD-HFD, choline-deficient high-fat diet; cDNA, complementary DNA; LPC, liver parenchymal cell; LPE, lysophosphatidylethanolamine; MASH, metabolic dysfunction–associated steatohepatitis; MASLD, metabolic dysfunction–associated steatotic liver disease; PC, phosphatidylcholine; PE, phosphatidylethanolamine; RT-PCR, real-time polymerase chain reaction; SD, standard diet; WD, Western diet; WT, Floxed wild-type littermates.

Mihael Vucur and Tom Luedde shared the last authorship.

Supplemental Digital Content is available for this article. Direct URL citations are provided in the HTML and PDF versions of this article on the journal's website, www.hepcommjournal.com.

This is an open access article distributed under the terms of the Creative Commons Attribution-Non Commercial-No Derivatives License 4.0 (http://creativecommons.org/licenses/by-nc-nd/4.0/), where it is permissible to download and share the work provided it is properly cited. The work cannot be changed in any way or used commercially without permission from the journal.
Copyright © 2025 The Author(s). Published by Wolters Kluwer Health, Inc. on behalf of the American Association for the Study of Liver Diseases.

Conclusions: Our analyses, therefore, suggest that loss of ACSL4 has no effect on the progression of MASLD induced by CD-HFD or the Western diet. The discrepancy between our and previously published results could be due to differences in the diets or the influence of a distinct microbiome, so the results obtained with hepatocyte-specific ACSL4^{LPC-KO} should be taken with caution.

Keywords: cell death, MAFLD, MASH, metabolic syndrome, NASH

INTRODUCTION

Obesity and its associated complications are a growing global public health challenge. As such, the incidence of metabolic dysfunction–associated steatotic liver disease (MASLD), as a hepatic manifestation of metabolic disease, has increased in recent years.[1,2] MASLD is defined as increased hepatic steatosis, either due to increased alcohol consumption or dietary fat intake. An increase in steatosis can result in liver damage and inflammation, which is known as metabolic dysfunction–associated steatohepatitis (MASH). If left untreated, this can progress to cirrhosis and HCC.[3] The therapeutic options available for these patients are severely limited. Only a minority of patients are able to achieve lifestyle modification with consequent loss of body weight.[4] In contrast, bariatric surgery is highly invasive and associated with complications.[5] Consequently, there is an urgent need for noninvasive therapeutic approaches. Despite considerable efforts that have been made in metabolic science in the past years, no drug has been approved for use in patients with MASLD. Programmed cell death has previously been linked to the pathogenesis of MASLD/MASH. However, preclinical studies on the best studied programmed cell death forms apoptosis[6,7] and necroptosis[8,9] showed contradictory results. Ferroptosis, a form of regulated necrotic cell death driven by iron-dependent lipid peroxidation, has been implicated in the pathogenesis of MASLD.[10]

The susceptibility of cells to ferroptosis is, among others, influenced by intracellular iron levels[11] and the composition of the lipid membrane, with high levels of polyunsaturated fatty acids in phospholipids promoting ferroptosis.[12,13] Patients with MASLD or MASH display elevated serum and liver iron levels, indicative of an increased ferroptosis sensitivity.[14] Furthermore, acyl-CoA synthetase long-chain member 4 (ACSL4), which may contribute to ferroptosis susceptibility by preferably activating long-chain polyunsaturated fatty acids that can then be esterified into phospholipids of cellular membranes,[12] is upregulated in patients with hepatic steatosis.[15] Based on this, it has recently been shown that the inhibition of ferroptosis through hepatocyte-specific knockout of ACSL4 in mice protects against developing obesity and associated steatosis when fed a high-fat/high-cholesterol/high-fructose diet (42% kcal fat, 42% kcal cholesterol with drinking water containing sucrose and fructose), a methionine-choline–deficient diet, or a high-fat diet (60% kcal fat).[16]

In the present study, we set out to investigate the effects of a conditional liver parenchymal cell (LPC)-specific ACSL4 knockout (ACSL4^{LPC-KO}) in mice fed with a choline-deficient high-fat diet (CD-HFD) and a Western diet (WD). These diets are known to efficiently recapitulate the key features of human metabolic syndrome, which encompasses weight gain and the development of glucose intolerance.[17] Notably, no differences were observed between ACSL4^{LPC-KO} and wild-type (WT) mice with regard to the development of MASLD or metabolic syndrome. Our findings, therefore, challenge the prevailing view on the involvement of ferroptosis in the development of MASLD and underscore the necessity of employing diverse dietary regimens in the quest for innovative therapeutic approaches.

METHODS

Mice

Acsl4$^{tm1a(EUCOMM)Wtsi}$ mice were obtained from Infrafrontier (EMMA strain EM:05887). These were subsequently crossed with Flp-deleter mice to remove the FRT-flanked lacZ/neomycin cassette to obtain mice only harboring the loxP-site–flanked Acsl4 alleles (designated *Acsl4*$^{tm1c(EUCOMM)Wtsi}$). Mice carrying LoxP-site–flanked alleles of Acsl4 were crossed to alfpAlb-Cre transgenic mice[18] that express the Cre recombinase regulated by both mouse albumin regulatory elements and α-fetoprotein enhancers to generate LPC-specific ablated mice. In all experiments, littermates carrying the respective loxP-flanked alleles but lacking expression of Cre recombinase were used as WT controls. The Cre recombinase is expressed in a hemizygous state. For 4-HNE staining, the liver of Alb-creERT2;Gpx4fl/fl mice on a standard diet (SD) 5 days after tamoxifen injection served as positive control.

For 4-HNE staining, the liver of tamoxifen-induced hepatocyte-specific GPX4 KO (Alb-creER^{T2};Gpx4$^{fl/fl}$) mice was used as a positive control 5 days after tamoxifen injection (GPX4$^{\Delta hep}$).[19]

Diet

In all experiments, 6-week-old male mice were fed a CD-HFD (Research Diets; D05010402), a WD (Research Diets; D16022301i), or an SD (Ssniff; V1534-30099) for varying time intervals as indicated. At the end of the feeding protocol, mice were fasted for at least 12 hours before being euthanized.

Glucose tolerance test

Mice were fasted overnight for 12 hours. On the next day, 2 mg of glucose per gram body weight was i.p. injected, and tail blood was taken at the indicated time points. Glucose levels were determined using a hand-held glucose analyzer (Contour XT Bayer) for the indicated time points.

Serum-analysis

Serum ALT, AST, GLDH, LDH, cholesterol, and triglycerides were measured by standard procedures in the Laboratory Diagnostic Center (LDZ) of the RWTH University Hospital Aachen.

RNA isolation and complementary DNA synthesis

RNA isolation and complementary DNA (cDNA) synthesis were conducted in accordance with the manufacturer's protocol using the RNeasy Mini Kit (Qiagen) for RNA isolation. The purity and concentration of the RNA were determined spectrophotometrically on the NanoDrop at an absorbance of 260 nm/280 nm. To obtain cDNA, 1 µg of RNA per experimental sample was processed with the QuantiTect cDNA Synthesis Kit (Qiagen) according to the manufacturer's instructions. For subsequent processing by real-time polymerase chain reaction (RT-PCR), the cDNA was diluted with nuclease-free water to a concentration of 10 ng/µL.

Oligonucleotides

The oligonucleotides were purchased from MWG Biotech and were used for quantitative expression analysis by PCR. According to the manufacturer's instructions, the oligonucleotides were dissolved in a solution of 100 pg/µL. For practical reaction application, the corresponding primer pairs were diluted again, resulting in a final concentration of 0.4 pg/µL. The sequences of the primers can be found in Supplemental Figure S3, http://links.lww.com/HC9/B962.

Quantitative real-time polymerase chain reaction

RT-PCR was conducted on the ViiA7 qRT-PCR system (Applied Biosystems/Thermo Fisher Scientific) in 96-well microtiter plates utilizing the oligonucleotide primers previously described. Each reaction batch comprised a total volume of 25 µL, comprising 1.2 µL cDNA (10 ng/µL), 12.5 µL GoTaq qPCR Master Mix (Promega), 9.3 µL nuclease-free H_2O, and 1 µL of each of the corresponding sense and antisense primers (10 pmol/µL). The PCR reaction cycles included a single step of 2 minutes at 50°C, an initial denaturation at 95°C for 10 minutes, followed by 40 cycles, each cycle consisting of 15 seconds at 95°C (denaturation) and 1 minute each at 60°C (annealing and elongation). A melting curve analysis was conducted for quality assurance purposes following each run, comprising 15 seconds at 95°C, 1 minute at 60°C, and 15 seconds at 95°C. For each experimental condition, 2 ΔCt values were determined by RT-PCR, and the arithmetic mean was calculated.

Western blot analysis

Liver tissue was homogenized in NP-40 lysis buffer using a tissue grind pestle (Kontes). Cell debris were removed by centrifugation for 10 minutes with 10,000 rpm and 4°C, thereby gaining protein lysates. These were resolved by reducing SDS-polyacrylamide gel electrophoresis, transferred to PVDF membrane and analyzed by immunoblotting as described.[20] Membranes were probed with anti-ACSL4 (Invitrogen) and anti-GAPDH (Bio-Rad). As secondary antibodies, HRP-conjugated anti-rabbit (ACSL4) and HRP-conjugated anti-mouse (GAPDH) were used.

Histological examination and evaluation

Liver tissue was fixed with paraformaldehyde (4%) and paraffin-embedded. Resulting paraffin sections (3 µm) were stained with hematoxylin and eosin or various primary and secondary antibodies, followed by diaminobenzidine staining. The following antibodies were used: antibodies against F4/80 (BMA Biomedicals AG, 1:120), B220 (BD Pharmingen, 1:3000), and CD3 (Zytomed, 1:250). The analysis was conducted using QuPath. 4-HNE staining was performed using VECTASTAIN Elite ABC-HRP Kit (PK-6101) and anti-4-HNE monoclonal antibody (HNEJ-2; Jaica, 1:200).

Frozen liver tissue was embedded in a tissue embedding medium and sectioned at a thickness of 15 µm using a cryostat. The sections were stained with Oil Red O (Sigma; O0625) following the manufacturer's protocol to visualize lipid content. Nuclear staining was performed by immersing the slides in hematoxylin solution (Sigma; GHS316) for 1 minute.

The histological scoring system for NAFLD, the old nomenclature of MASLD, was performed according to the NAS scoring system.[21]

Liquid chromatography-mass spectrometry

Extracts of mouse liver tissue samples (ca. 50 mg) were dried under nitrogen after being dissolved and homogenized in 1 mL ethanol/PBS (85%/15%) by precellys ceramic beads (CK 14S) using the Minilys homogenizer (Bertin Technologies). The dried extracts were dissolved in 1 mL solvent mixture (acetonitrile/2-propanol; 1/1). For tandem mass spectrometric analysis (QTRAP 5500, sciex), the SPLASH Lipidomix Mass Spec Standard (Avanti) includes the isotopically labeled internal standards of the lipid classes and was added to the samples before extraction. A flow injection analysis method and an isocratic mode were used. The mobile phase consisted of acetonitrile/2-propanol/dichloromethane (45:45:10, vol/vol/vol). An analytical UHPLC (ExcionLC AD; sciex) was coupled to MS/MS. The lipid classes PE and lysophosphatidylethanolamine (LPE) were measured by a neutral loss scan of 141 *m/z*, and phosphatidylcholine (PC) and LPC were measured by a precursor ion scan of 184 *m/z*. The following mass ranges were chosen: 580–880 *m/z* for PE, 380–580 *m/z* for LPE, 600–900 *m/z* for PC, and 400–600 *m/z* for LPC. Positive ionization mode was performed for the lipid analysis. The software LipidView (V1.2; Sciex) was used for the identification and quantification of the detected lipid compounds.[22]

Ethics approval

All animal experiments were approved by the Federal Ministry for Nature, Environment and Consumers' Protection of the state of North Rhine-Westphalia and were performed in accordance to the respective national, federal, and institutional regulations. The authors confirm that all experiments were done in accordance to the ARRIVE guidelines.

Statistical analysis and general experimental design

The data were analyzed using PRISM software (GraphPad Prism 8 Software, Inc.) and are expressed as the mean with SD if indicated. The statistical significance between the experimental groups was assessed using an unpaired 2-sample *t* test and a Mann-Whitney test.

RESULTS

ACSL4^{LPC-KO} fails to provide protection against the development of metabolic syndrome on CD-HFD

To study the effect of ferroptosis inhibition in MASLD, we deleted the pro-ferroptotic regulator ACSL4 specifically in liver parenchymal cells (ACSL4^{LPC-KO}) (Figure 1A). As expected, ACSL4^{LPC-KO} mice exhibited specific alterations in the lipid profile of whole liver tissue, including the accumulation of lysophosphatidylcholine 16:0 and LPE 16:0 and 18:0, revealing a functional knockout[23] (Figure 1A and Supplemental Figure S1, http://links.lww.com/HC9/B962). To functionally dissect the specific outcome of impaired ferroptosis in MASLD, ACSL4^{LPC-KO} and WT littermates were fed with CD-HFD for either 20 or 40 weeks. As shown in Figure 1C, CD-HFD feeding resulted in weight gain over the 20-week and 40-week feeding period. However, no differences were observed between ACSL4^{LPC-KO} and WT mice in terms of relative weight gain or absolute weight (Figures 1C, D). This was also accompanied by a similar weekly feed intake (Figure 1E).

Since obesity and MASLD often is accompanied by the development of type II diabetes, we next examined the impact of ACSL4^{LPC-KO} in glucose tolerance test under CD-HFD. CD-HFD resulted in impaired glucose tolerance compared to mice fed an SD. In accordance with the previously observed outcomes, the deletion of ACSL4 did not improve glucose tolerance in either the 20-week feeding group (Figure 1F) or the 40-week feeding group (Figure 1G).

To summarize, the knockout of *Acsl4* in liver parenchymal cells does not protect against diet-induced weight gain and its consequences.

ACSL4^{LPC-KO} does not protect mice from developing MASLD and associated hepatic injury

As described above, CD-HFD not only leads to weight gain and the development of metabolic syndrome but also to MASLD with subsequent liver damage. To investigate the influence of liver parenchymal cell–specific knockout of *Ascl4* on the development of MASLD with progression to MASH, we further characterized the hepatic phenotype of mice under CD-HFD. Macroscopic and histopathological examination of the liver showed pronounced steatosis, but no differences between ACSL4^{LPC-KO} and WT mice after 20 and 40

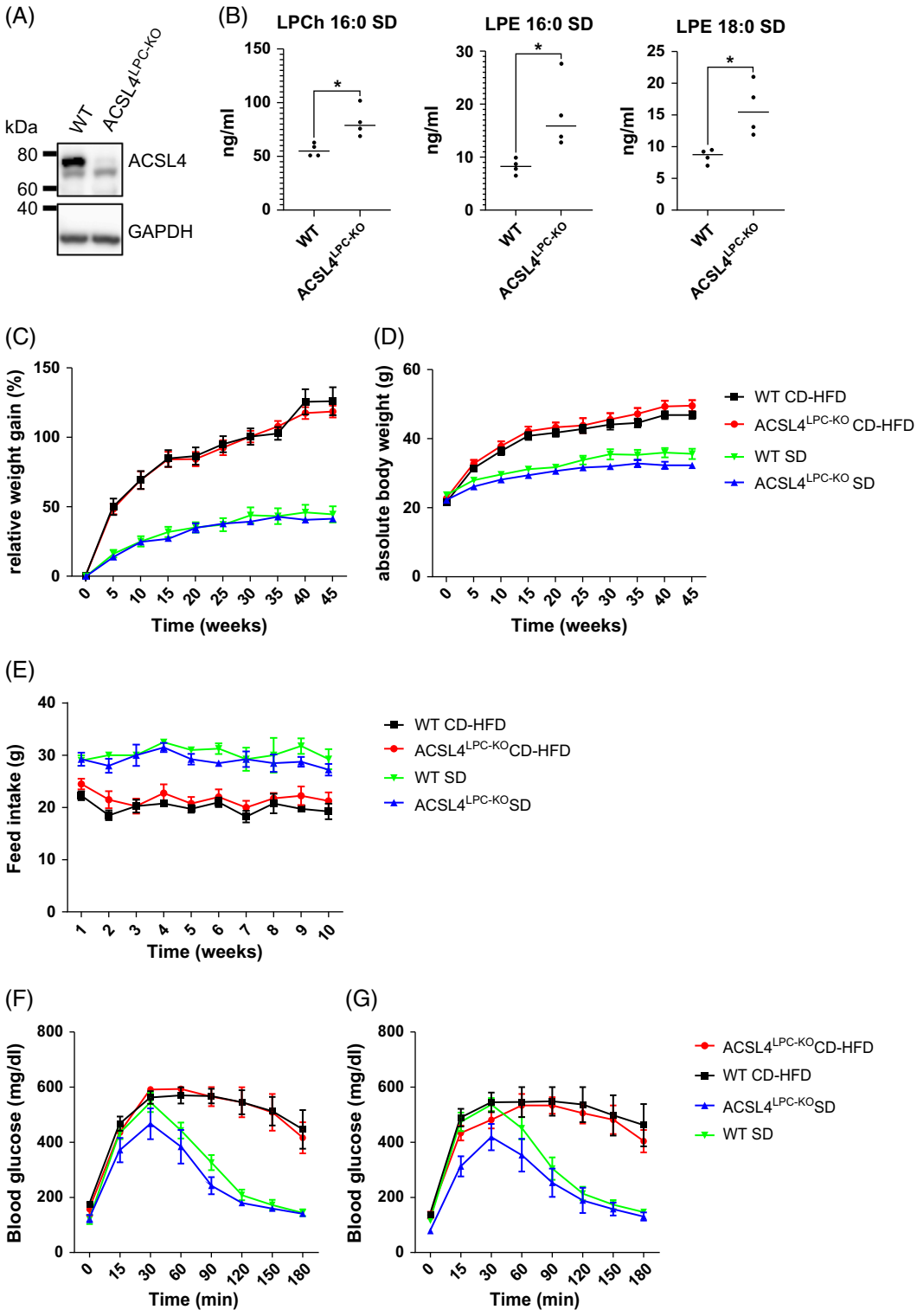

FIGURE 1 ACSL4^{LPC-KO} has no impact on weight gain and glucose tolerance under CD-HFD. (A) ACSL4 protein levels in the livers of ACSL4^{LPC-KO} and loxP-flanked control mice fed normal chow were assessed by Western blot. (B) ACSL4^{LPC-KO} resulted in distinct alterations in the lipid profile of whole liver tissue in LPCh and LPE species, as measured through LC/MS. (C, D) ACSL4^{LPC-KO} showed similar weight gain compared to WT under CD-HFD over the indicated time period, both in terms of relative weight gain (C) and absolute weight (D). (E) Feed intake was lower in CD-HFD than in SD, but did not differ between ACSL4^{LPC-KO} and WT. (F, G) CD-HFD led to impaired glucose tolerance compared to SD measured by glucose tolerance tests. In 20-week-old (F) and 40-week-old mice (G) fed with indicated diets, no difference between ACSL4^{LPC-KO} and WT was observed. Mann-Whitney U test, * for $p \leq 0.05$. Abbreviations: ACSL4^{LPC-KO}, liver parenchymal cell–specific deletion of pro-ferroptotic gene acyl-CoA synthetase long-chain family member 4; CD-HFD, choline-deficient high-fat diet; LC-MS, liquid chromatography-mass spectrometry; LPCh, lysophosphatidylcholine; LPE, lysophosphatidylethanolamine; SD, standard diet; WT, wild-type.

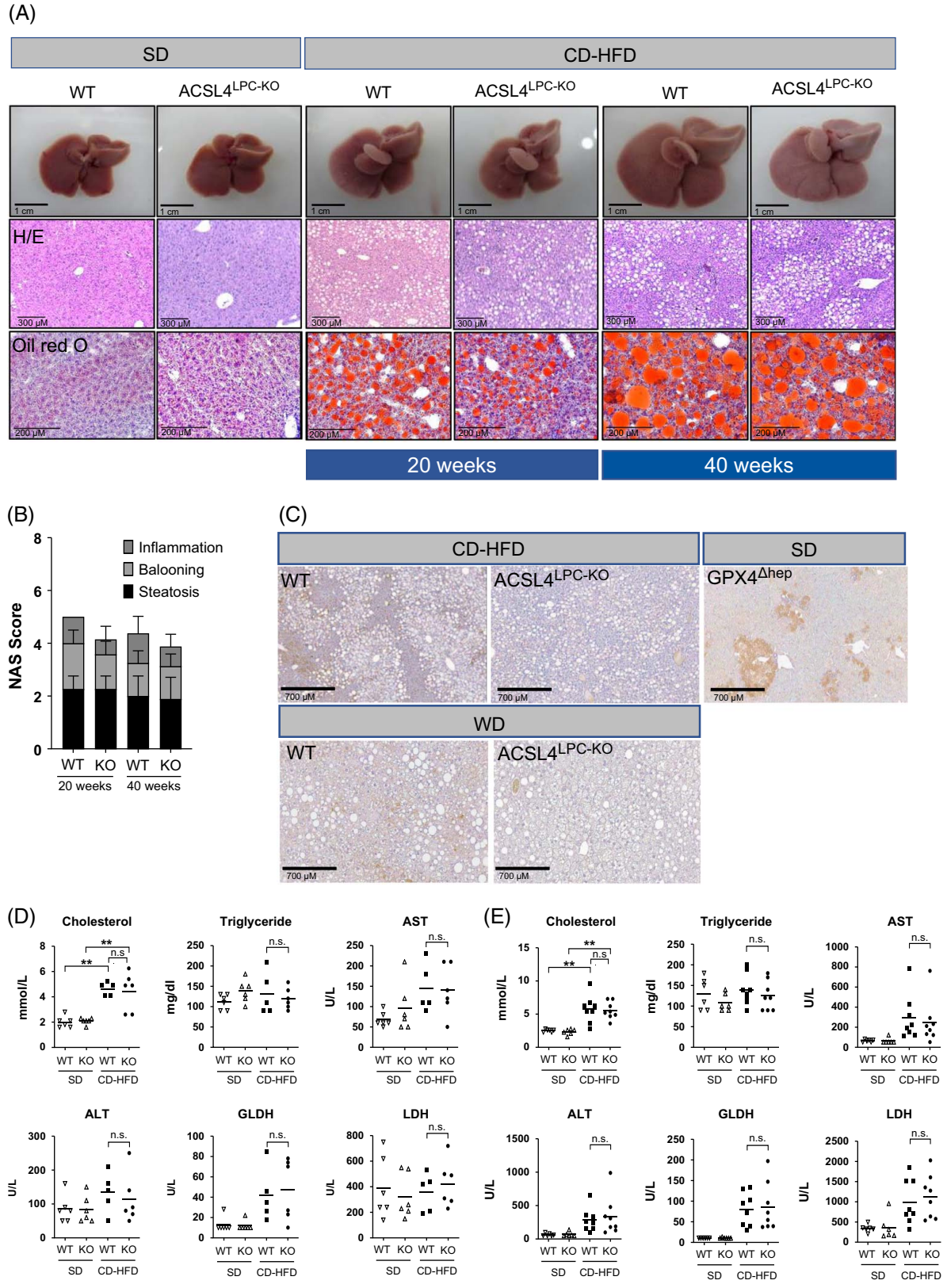

FIGURE 2 ACSL4^{LPC-KO} does not protect against liver injury or the development of MASLD, despite providing protection against lipid peroxidation. (A) ACSL4^{LPC-KO} mice and WT mice both develop steatosis hepatitis after 20 and 40 weeks of feeding. (b) No difference between ACSL4^{LPC-KO} and WT in the development of steatohepatitis was observed in the NAS score on histology in 20-week-old and 40-week-old mice. (C) As indicated by 4-HNE staining, pronounced lipid peroxidation was detected in WT mice compared to ACSL4^{LPC-KO} mice when fed a CD-HFD for 40 weeks and a WD for 20 weeks. The liver of tamoxifen-induced hepatocyte-specific GPX4 KO (Alb-creER^{T2};Gpx4$^{fl/fl}$) mice was used as a

positive control 5 days after tamoxifen injection (GPX4$^{\Delta hep}$). (D, E) After 20 weeks (D) and 40 weeks (E), the CD-HFD led to an increase in serum values showing liver damage (AST, ALT, GLDH, and LDH) and aberrant parameters of lipid metabolism (cholesterol) as indicated. No difference could be detected between ACSL4^{LPC-KO} and WT mice. Mann-Whitney U test, ** for $p \leq 0.01$. Abbreviations: ACSL4^{LPC-KO}, liver parenchymal cell–specific deletion of pro-ferroptotic gene acyl-CoA synthetase long-chain family member 4; CD-HFD, choline-deficient high-fat diet; MASLD, metabolic dysfunction–associated steatotic liver disease; WD, Western diet; WT, wild-type.

weeks of CD-HFD were observed (Figure 2A). In line, the NAS score also demonstrated no differences between the 2 groups (Figure 2B). Importantly, 4-hydroxynonenal, a highly toxic aldehyde product of lipid peroxidation recently validated as a specific in vivo marker for ferroptosis induction,[24,25] was increased in livers of WT mice compared to ACSL4^{LPC-KO} mice (Figure 2C). The liver of tamoxifen-induced hepatocyte-specific GPX4 KO (Alb-creER^{T2};Gpx4$^{fl/fl}$) mice was used as a positive control 5 days after tamoxifen injection (GPX4$^{\Delta hep}$). Furthermore, serum cholesterol and triglyceride levels were found to be similar in WT and ASCL4^{LPC-KO} mice (Figures 2D, E). Since the progression of MASLD to MASH is associated with liver damage, we next measured the serum parameters for liver injury (AST, ALT, and GLDH) in mice fed with CD-HFD and SD. While CD-HFD was associated with mild hepatitis, there were also no differences between ACSL4^{LPC-KO} and WT mice in the group of 20 weeks and 40 weeks of feeding (Figures 2D, E).

Together, both ACSL4^{LPC-KO} and WT mice developed diet-induced liver damage as defined by MASLD or MASH to the same extent.

ACSL4^{LPC-KO} mitigates inflammation and fibrogenesis induced by CD-HFD

As the progression of MASLD to MASH in humans is accompanied by intrahepatic inflammation with an accumulation of immune cells, we further sought to characterize inflammation upon CD-HFD feeding. It has already been described that the infiltration of different immune cells, particularly lymphocytes, contributes to the phenotype observed in CD-HFD.[17] Of note, we could not detect differences between ACSL4^{LPC-KO} and WT mice regarding the amount of infiltrating CD3^{+} T lymphocytes, cytotoxic CD8+ T cells or CD4+ T-helper cells, B220^{+} B lymphocytes, or F4/80^{+} macrophages (Figures 3A–C and Supplemental Figure S2, http://links.lww.com/HC9/B962). We further examined the expression of the indicated cytokines and alarmins in the whole liver tissue of mice fed with CD-HFD. Again, no differences in hepatic inflammation induced by CD-HFD between ACSL4^{LPC-KO} and WT mice could be observed (Figure 3D).

Since both Duan et al paper and similar studies[16,23] have shown that ACSL4 alters the expression of genes associated with hepatic fibrogenesis and hepatic lipid deposition, we next examined the extent to which the expression of selected genes differs between KO and WT mice in our diet model. The expression levels of fibrosis- and lipid-deposition–associated genes were examined using quantitative RT-PCR, which once again demonstrated that genes promoting hepatic fibrogenesis and hepatic lipid deposition were not significantly down-regulated in ACSL4^{LPC-KO} mice compared to WT mice (Figure 3E).

Taken together, these findings suggest that ACSL4^{LPC-KO} in our dietary model does not affect hepatic inflammation, fibrogenesis, or lipid metabolism in the progression of MASLD and MASH.

ACSL4^{LPC-KO} does not provide protection against weight gain when mice are subjected to WD

To exclude the possibility of a methodological effect, WT and ACSL4^{LPC-KO} mice were subjected to a WD, which also resulted in weight gain and the development of a metabolic syndrome. However, as illustrated in Figure 4, the ACSL4^{LPC-KO} does not confer protection against weight gain, whether assessed in absolute or relative terms and was not different from the WT littermates.

DISCUSSION

Ferroptosis is characterized by an iron-dependent, unrestrained generation of lipid hydroperoxides in cellular membranes, which subsequently leads to membrane deterioration, membrane rupture, and cell death.[26] ACSL4 may increase the cell's susceptibility to ferroptosis, as it preferably activates long-chain polyunsaturated fatty acids (namely arachidonic acid and adrenic acid) which upon esterification into phospholipids by another class of enzymes may undergo peroxidation, thereby contributing to phospholipid autooxidation and cell membrane rupture.[12] Interestingly, arachidonic acid has been demonstrated to be upregulated in mice fed a methionine-choline–deficient diet suggesting therapeutic potential in modulating ferroptosis in MASLD.[27]

Indeed, pharmacological ferroptosis inhibitors (eg, ferrostatin-1, liproxstatin-1, or Trolox) mitigate MASLD and inflammation-associated MASH progression in mice.[27–30] Moreover, rosiglitazone, a PPARγ agonist and approved drug for the treatment of diabetes mellitus, exerts its effect by inhibiting ACSL4 (as an off-target effect) and ferroptosis, leading to weight loss,

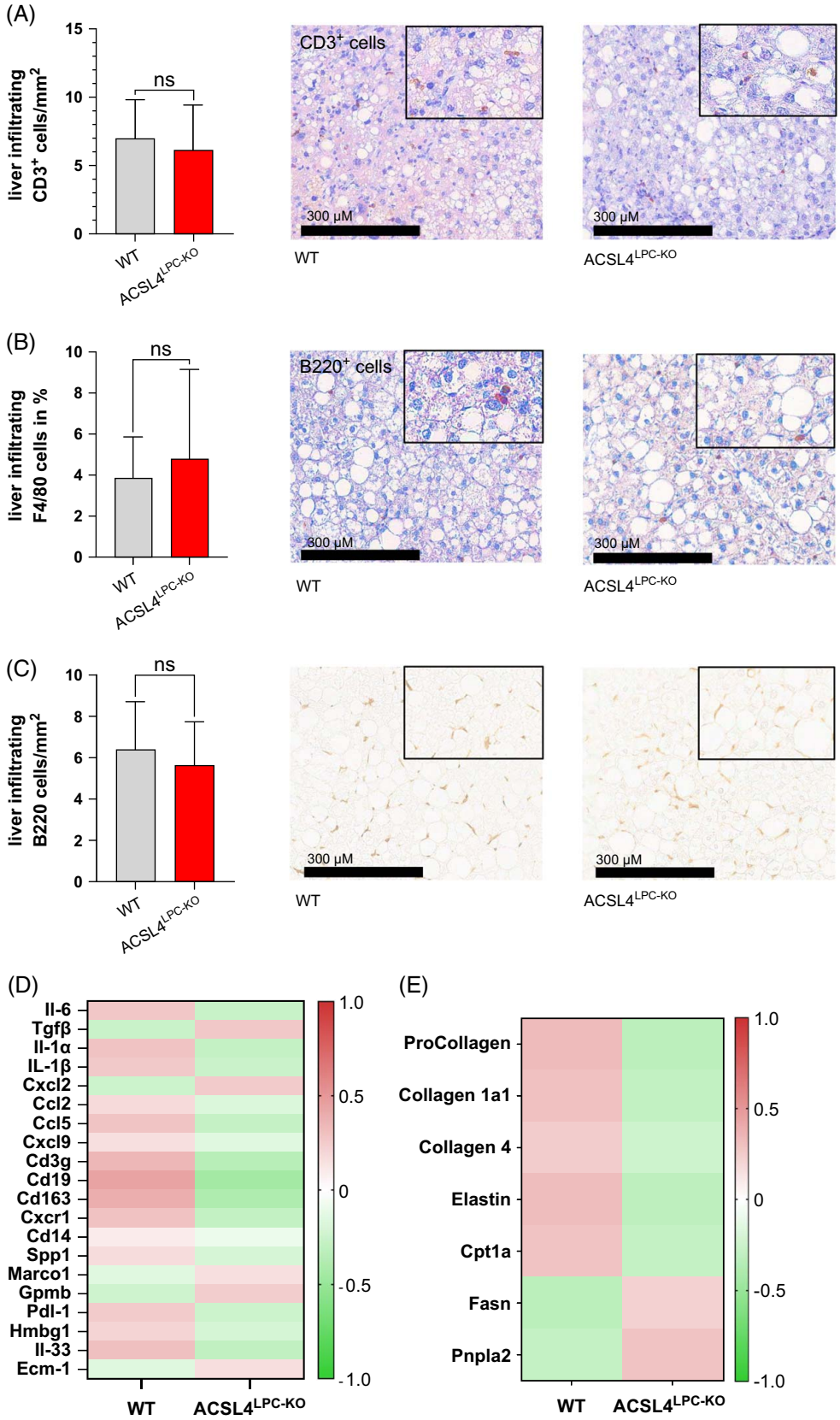

FIGURE 3 qPCR-based and immunohistochemical examinations showed no differences between ACSL4^{LPC-KO} and WT in terms of tissue inflammation and fibrogenesis. (A–C) Immunohistochemical staining did not show any significant differences of CD3^{+} T cells (A), B220^{+} B cells (B), and F4/80^{+} cells (C) between the liver of ACSL4^{LPC-KO} and WT mice fed with a CD-HFD for 40 weeks. (D) qPCR-based studies indicated no

differences in inflammatory parameters (cytokines, distinct receptors, and alarmins) between ACSL4^{LPC-KO} and WT mice fed with the CD-HFD for 40 weeks. (E) Analysis of distinct fibrogenesis and fat metabolism–associated genes in whole liver tissue after 40 weeks of CD-HFD showed no difference between WT and ACSL4^{LPC-KO}. Abbreviations: ACSL4^{LPC-KO}, liver parenchymal cell–specific deletion of pro-ferroptotic gene acyl-CoA synthetase long-chain family member 4; CD-HFD, choline-deficient high-fat diet; WT, wild-type.

and it has been described to ameliorate arsenic-induced steatohepatitis in mice.[31–34] Examining the distinct role of ACSL4 in the progression of MASLD, Duan et al challenged ACSL4^{LPC-KO} and WT mice with 3 different diets to induce the development of MASLD and metabolic syndrome: (i) high-fat, high-cholesterol, and high-fructose diet, (ii) methionine-choline–deficient diet, and (iii) high-fat diet. They found that ACSL4^{LPC-KO} mice show increased mitochondrial respiration and

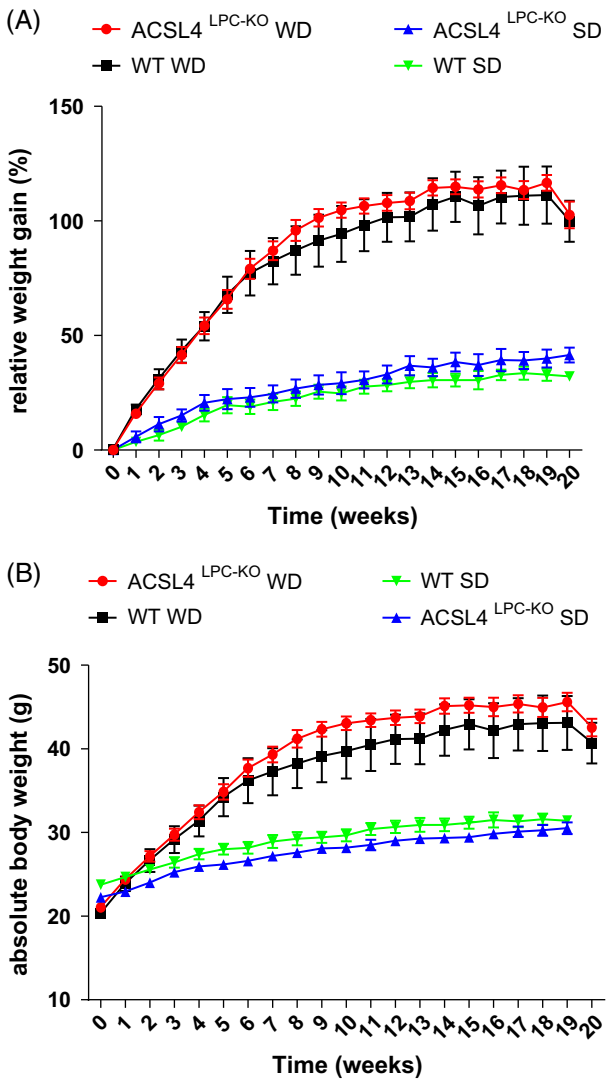

FIGURE 4 ACSL4^{LPC-KO} does not influence weight gain under the Western diet. (A, B) ACSL4^{LPC-KO} showed similar weight gain compared to WT under CD-HFD over the indicated time period, both in terms of relative weight gain (A) and absolute weight (B). Abbreviations: ACSL4^{LPC-KO}, liver parenchymal cell–specific deletion of pro-ferroptotic gene acyl-CoA synthetase long-chain family member 4; CD-HFD, choline-deficient high-fat diet; WT, wild-type.

β-oxidation with increased catabolic fatty acid metabolism, which protected against MASLD and metabolic syndrome.[16]

In this work, we first challenged the role of ACSL4 in the same ACSL4^{LPC-KO} mouse model when subjected to CD-HFD. The CD-HFD induces steatosis, inflammation, mild fibrosis, and weight gain when fed over 10 weeks.[35]

Unexpectedly, we did not observe a protective effect in ACSL4^{LPC-KO} mice with regard to the development of MASLD or weight gain. Moreover, there were no differences in hepatic injury, cholesterol metabolism, or glucose tolerance. These contrasting results raise the question of the underlying causes.

To rule out the possibility that the lack of a discernible phenotype was due to a nonfunctional knockout of ACSL4, we conducted a functional validation of the knockout. We performed a mass spectrometry–based lipidomic analysis to identify alterations in ACSL4-related lipids. Consistent with existing literature,[23] we observed an accumulation of LPC 16:0, as well as LPE 16:0 and 18:0 (Figure 1B). One methodological aspect of the study by Duan et al is the unclear regulation of Cre recombinase, as no information was available on transgene integration or Cre expression status (heterozygous or homozygous), which could have influenced the phenotype. Moreover, it is well established that variations in genetic background, potential influences from the microbiome, or differences in husbandry conditions across various animal facilities may contribute to disparate phenotypes.[36,37] However, to exclude the possibility of a diet-related influence, a secondary dietary regimen was implemented, which was not used in the study by Duan et al. The WD has been shown to induce weight gain and liver fibrosis, particularly when consumed over extended periods.[38,39] In line with the CD-HFD model, no differential outcomes were identified between WT and ACSL4^{LPC-KO} mice in the WD model (Figure 4), suggesting that the diet is unlikely to be the primary cause of the observed disparities between both studies.

As we examined the role of ACSL4^{LPC-KO} under CH-HFD, it should be noted that investigating ferroptosis in a CD-HFD model may present certain challenges. In line, a previous study has shown that deferoxamine, a common ferroptosis inhibitor, was unable to mitigate liver injury in mice fed a CD-HFD with ethanol.[27] In contrast, 2 other ferroptosis inhibitors were found to inhibit cell death and inflammation in the same dietary model: Trolox, a derivative of vitamin E, and deferiprone, an iron chelator.[27] In this context, it could be suggested that a

choline-deficient diet limits the synthesis of PC, which is a driver of ferroptosis, and thus reduces the protective effect of ACSL4^{LPC-KO}. However, it has been already shown that dietary choline deficiency does not lead to a decrease in hepatic PC in mice.[40]

Another hallmark of a CD-HFD is the absence of an increase in serum triglycerides, as evidenced in this study (Figures 2D, E). This phenomenon is attributed to impaired synthesis of VLDL due to choline deficiency. Consequently, the disruption of VLDL synthesis leads to the accumulation of triglycerides within the liver, ultimately resulting in the development of steatosis.[41]

Moreover, it is worth mentioning that the observed weight gain in the CD-HFD exceeded the weight gain observed in the work of Duan et al[16] when fed a high-fat diet (HFD) and HFD with added sucrose and fructose in the drinking water, although the fat content in the diets was comparable or even less (60% and 42% vs. 45% for CD-HFD). In this regard, it is important to highlight that the absence of choline per se does not result in an increase in body weight.[42] In summary, it can be concluded that the choice of diet cannot explain the differing phenotypes.

The progression from MASLD to MASH, cirrhosis, and eventually HCC is driven by increased intrahepatic inflammation.[17,43] Given that ferroptosis, as a lytic form of cell death, leads to immune activation,[44,45] and that ferroptosis inhibitors have been shown to alleviate inflammatory damage in mice,[28] we hypothesized that ACSL4^{LPC-KO} would attenuate hepatic inflammation and subsequent fibrogenesis. However, even though lymphocytes and macrophages are known to be primary cells involved in the pathogenesis of MASH,[43,46] no differences were detected in the investigated cell types (Figures 3A–C; Supplemental Figure S2, http://links.lww.com/HC9/B962). Moreover, the expression of distinct cytokines known to be involved in MASH development, fibrogenesis, and lipid metabolism[16,23] was unaffected by ACSL4^{LPC-KO} (Figures 3D, E).

In conclusion, our study shows that the targeted deletion of ACSL4 in LPC in mice fed a CD-HFD or WD has no effect on the formation of a metabolic syndrome, the development of MASLD, or, in the case of CD-HFD, the inflammation and fibrogenesis that are decisive for the progression to liver cirrhosis.

The exact reasons for these contradictory results of our work and that of Duan et al remain elusive. However, the discrepant results warrant careful consideration of the experimental conditions, such as animal husbandry and the choice of diet used.

DATA AVAILABILITY STATEMENT

The data sets used and analyzed during the current study are available from the corresponding author upon reasonable request.

AUTHOR CONTRIBUTIONS

Carolin Angendohr, Mihael Vucur, and Tom Luedde designed and guided the research. Carolin Angendohr, Mihael Vucur, and Tom Luedde wrote the manuscript with help from other authors. Carolin Angendohr and Christiane Koppe performed and analyzed most of the experiments. Anne T. Schneider, Leonie Keysberg, Michael T. Singer, Marcus Conrad, Johannes G. Bode, Julian Gilljam, Sebastian Doll, and Diran Herebian contributed to the research design and/or conducted experiments. Marcus Conrad and Sebastian Doll provided the mouse model. All authors read and agreed on the content of the paper.

FUNDING INFORMATION

Tom Luedde was funded by the European Research Council (ERC): grant agreement 771083; the German Research Foundation (DFG): 279874820, 461704932, 440603844; the German Cancer Aid (Deutsche Krebshilfe): 70114893, 70115166; and in part by the Ministry of Culture and Science of the State of North Rhine-Westphalia: NW21-062E (CANTAR), PROFILNRW-2020-107-A (MODS), and the German Federal Ministry of Education and Research: 031L0312B (Transform-Liver). Mihael Vucur was supported by the German Cancer Aid (Deutsche Krebshilfe): 70114893 and the Ministry of Culture and Science of the State of North Rhine-Westphalia: NW21-062E (CANTAR). Johannes G. Bode was supported by the LiSyM Cancer Network C-TIP HCC (031L0257G), funded by the German Federal Ministry of Education and Research. Carolin Angendohr was funded by the DFG-funded Clinician Scientist Program FUTURE-4-CSPMM: 493659010. Marcus Conrad received funding from the DFG (CO 291/7-1), the Priority Program SPP 2306 (CO 291/9-1, 461385412; CO 291/10-1, 461507177), the CRC TRR 353 (CO 291/11-1; 471011418), the German Federal Ministry of Education and Research (BMBF) FERRO-PATH (01EJ2205B) and the European Research Council (ERC) under the European Union's Horizon 2020 research and innovation program (grant agreement no. GA 884754).

CONFLICTS OF INTEREST

Marcus Conrad is cofounder and shareholder of ROSCUE Therapeutics GmbH. The remaining authors have no conflicts to report.

DECLARATION OF AI AND AI-ASSISTED TECHNOLOGIES IN THE WRITING PROCESS

During the preparation of this work, the authors used Grammarly and ChatGPT 4o to correct the grammar, clarity, and conciseness of the text. After using this tool, the authors reviewed and edited the content as needed and take full responsibility for the content of the published article.

REFERENCES

1. Liu J, Ayada I, Zhang X, Wang L, Li Y, Wen T, et al. Estimating global prevalence of metabolic dysfunction-associated fatty liver disease in overweight or obese adults. Clin Gastroenterol Hepatol. 2022;20:e573–82.
2. Zhang X, Wu M, Liu Z, Yuan H, Wu X, Shi T, et al. Increasing prevalence of NAFLD/NASH among children, adolescents and young adults from 1990 to 2017: A population-based observational study. BMJ Open. 2021;11:e042843.
3. Zeng J, Fan JG, Francque SM. Therapeutic management of metabolic dysfunction associated steatotic liver disease. United European Gastroenterol J. 2024;12:177–86.
4. Wing RR, Phelan S. Long-term weight loss maintenance. Am J Clin Nutr. 2005;82(1 suppl):222S–25SS.
5. Chang SH, Stoll CR, Song J, Varela JE, Eagon CJ, Colditz GA. The effectiveness and risks of bariatric surgery: An updated systematic review and meta-analysis, 2003-2012. JAMA Surg. 2014;149:275–87.
6. Gautheron J, Vucur M, Reisinger F, Cardenas DV, Roderburg C, Koppe C, et al. A positive feedback loop between RIP3 and JNK controls non-alcoholic steatohepatitis. EMBO Mol Med. 2014;6: 1062–74.
7. Hatting M, Zhao G, Schumacher F, Sellge G, Al Masaoudi M, Gabetaler N, et al. Hepatocyte caspase-8 is an essential modulator of steatohepatitis in rodents. Hepatology. 2013;57: 2189–201.
8. Gautheron J, Vucur M, Schneider AT, Severi I, Roderburg C, Roy S, et al. The necroptosis-inducing kinase RIPK3 dampens adipose tissue inflammation and glucose intolerance. Nat Commun. 2016;7:11869.
9. Preston SP, Stutz MD, Allison CC, Nachbur U, Gouil Q, Tran BM, et al. Epigenetic silencing of RIPK3 in hepatocytes prevents MLKL-mediated necroptosis from contributing to liver pathologies. Gastroenterology. 2022;163:1643–657 e14.
10. Zhang H, Zhang E, Hu H. Role of ferroptosis in non-alcoholic fatty liver disease and its implications for therapeutic strategies. Biomedicines. 2021;9:1660.
11. Wang H, An P, Xie E, Wu Q, Fang X, Gao H, et al. Characterization of ferroptosis in murine models of hemochromatosis. Hepatology. 2017;66:449–65.
12. Doll S, Proneth B, Tyurina YY, Panzilius E, Kobayashi S, Ingold I, et al. ACSL4 dictates ferroptosis sensitivity by shaping cellular lipid composition. Nat Chem Biol. 2017;13:91–8.
13. Mortensen MS, Ruiz J, Watts JL. Polyunsaturated fatty acids drive lipid peroxidation during ferroptosis. Cells. 2023; 12:804.
14. Wang H, Sun R, Yang S, Ma X, Yu C. Association between serum ferritin level and the various stages of non-alcoholic fatty liver disease: A systematic review. Front Med (Lausanne). 2022; 9:934989.
15. Westerbacka J, Kolak M, Kiviluoto T, Arkkila P, Siren J, Hamsten A, et al. Genes involved in fatty acid partitioning and binding, lipolysis, monocyte/macrophage recruitment, and inflammation are overexpressed in the human fatty liver of insulin-resistant subjects. Diabetes. 2007;56: 2759–65.
16. Duan J, Wang Z, Duan R, Yang C, Zhao R, Feng Q, et al. Therapeutic targeting of hepatic ACSL4 ameliorates NASH in mice. Hepatology. 2022;75:140–53.
17. Wolf MJ, Adili A, Piotrowitz K, Abdullah Z, Boege Y, Stemmer K, et al. Metabolic activation of intrahepatic CD8+ T cells and NKT cells causes nonalcoholic steatohepatitis and liver cancer via cross-talk with hepatocytes. Cancer Cell. 2014; 26:549–64.
18. Kellendonk C, Opherk C, Anlag K, Schutz G, Tronche F. Hepatocyte-specific expression of Cre recombinase. Genesis. 2000;26:151–3.
19. Mishima E, Ito J, Wu Z, Nakamura T, Wahida A, Doll S, et al. A non-canonical vitamin K cycle is a potent ferroptosis suppressor. Nature. 2022;608:778–83.
20. Schneider AT, Gautheron J, Feoktistova M, Roderburg C, Loosen SH, Roy S, et al. RIPK1 suppresses a TRAF2-dependent pathway to liver cancer. Cancer Cell. 2017;31: 94–109.
21. Kleiner DE, Brunt EM, Van Natta M, Behling C, Contos MJ, Cummings OW, et al. Design and validation of a histological scoring system for nonalcoholic fatty liver disease. Hepatology. 2005;41:1313–21.
22. Ozbalci C, Sachsenheimer T, Brugger B. Quantitative analysis of cellular lipids by nano-electrospray ionization mass spectrometry. Methods Mol Biol. 2013;1033:3–20.
23. Singh AB, Kan CFK, Kraemer FB, Sobel RA, Liu J. Liver-specific knockdown of long-chain acyl-CoA synthetase 4 reveals its key role in VLDL-TG metabolism and phospholipid synthesis in mice fed a high-fat diet. Am J Physiol Endocrinol Metab. 2019;316: E880–94.
24. Chen X, Huang J, Yu C, Liu J, Gao W, Li J, et al. A noncanonical function of EIF4E limits ALDH1B1 activity and increases susceptibility to ferroptosis. Nat Commun. 2022;13:6318.
25. Podszun MC, Chung JY, Ylaya K, Kleiner DE, Hewitt SM, Rotman Y. 4-HNE immunohistochemistry and image analysis for detection of lipid peroxidation in human liver samples using vitamin E treatment in NAFLD as a proof of concept. J Histochem Cytochem. 2020;68:635–43.
26. Dixon SJ, Olzmann JA. The cell biology of ferroptosis. Nat Rev Mol Cell Biol. 2024;25:424–42.
27. Tsurusaki S, Tsuchiya Y, Koumura T, Nakasone M, Sakamoto T, Matsuoka M, et al. Hepatic ferroptosis plays an important role as the trigger for initiating inflammation in nonalcoholic steatohepatitis. Cell Death Dis. 2019;10:449.
28. Qi J, Kim JW, Zhou Z, Lim CW, Kim B. Ferroptosis affects the progression of nonalcoholic steatohepatitis via the modulation of lipid peroxidation-mediated cell death in mice. Am J Pathol. 2020;190:68–81.
29. Li X, Wang TX, Huang X, Li Y, Sun T, Zang S, et al. Targeting ferroptosis alleviates methionine-choline deficient (MCD)-diet induced NASH by suppressing liver lipotoxicity. Liver Int. 2020; 40:1378–94.
30. Li S, Zhuge A, Wang K, Xia J, Wang Q, Han S, et al. Obeticholic acid and ferrostatin-1 differentially ameliorate non-alcoholic steatohepatitis in AMLN diet-fed ob/ob mice. Front Pharmacol. 2022;13:1081553.
31. Wei S, Qiu T, Wang N, Yao X, Jiang L, Jia X, et al. Ferroptosis mediated by the interaction between Mfn2 and IREalpha promotes arsenic-induced nonalcoholic steatohepatitis. Environ Res. 2020;188:109824.
32. Brunani A, Caumo A, Graci S, Castagna G, Viberti G, Liuzzi A. Rosiglitazone is more effective than metformin in improving fasting indexes of glucose metabolism in severely obese, non-diabetic patients. Diabetes Obes Metab. 2008;10:460–7.
33. Askari B, Kanter JE, Sherrid AM, Golej DL, Bender AT, Liu J, et al. Rosiglitazone inhibits acyl-CoA synthetase activity and fatty acid partitioning to diacylglycerol and triacylglycerol via a peroxisome proliferator-activated receptor-gamma-independent mechanism in human arterial smooth muscle cells and macrophages. Diabetes. 2007;56:1143–52.
34. Merkel M, Goebel B, Boll M, Adhikari A, Maurer V, Steinhilber D, et al. Mitochondrial reactive oxygen species formation determines ACSL4/LPCAT2-mediated ferroptosis. Antioxidants (Basel). 2023;12:1590.
35. Radhakrishnan S, Ke JY, Pellizzon MA. Targeted nutrient modifications in purified diets differentially affect nonalcoholic fatty liver disease and metabolic disease development in rodent models. Curr Dev Nutr. 2020;4:nzaa078.

36. Ericsson AC, Franklin CL. The gut microbiome of laboratory mice: Considerations and best practices for translational research. Mamm Genome. 2021;32:239–50.
37. Russell LN, Hyatt WS, Gannon BM, Simecka CM, Randolph MM, Fantegrossi WE. Effects of laboratory housing conditions on core temperature and locomotor activity in mice. J Am Assoc Lab Anim Sci. 2021;60:272–80.
38. Zheng C, Snow BE, Elia AJ, Nechanitzky R, Dominguez-Brauer C, Liu S, et al. Tumor-specific cholinergic CD4(+) T lymphocytes guide immunosurveillance of hepatocellular carcinoma. Nat Cancer. 2023;4:1437–54.
39. Gallage S, Ali A, Barragan Avila JE, Seymen N, Ramadori P, Joerke V, et al. A 5:2 intermittent fasting regimen ameliorates NASH and fibrosis and blunts HCC development via hepatic PPARalpha and PCK1. Cell Metab. 2024;36: 1371–93 e7.
40. Kulinski A, Vance DE, Vance JE. A choline-deficient diet in mice inhibits neither the CDP-choline pathway for phosphatidylcholine synthesis in hepatocytes nor apolipoprotein B secretion. J Biol Chem. 2004;279:23916–24.
41. Cole LK, Vance JE, Vance DE. Phosphatidylcholine biosynthesis and lipoprotein metabolism. Biochim Biophys Acta. 2012;1821: 754–61.
42. Raubenheimer PJ, Nyirenda MJ, Walker BR. A choline-deficient diet exacerbates fatty liver but attenuates insulin resistance and glucose intolerance in mice fed a high-fat diet. Diabetes. 2006; 55:2015–20.
43. Caballero T, Gila A, Sanchez-Salgado G, Munoz de Rueda P, Leon J, Delgado S, et al. Histological and immunohistochemical assessment of liver biopsies in morbidly obese patients. Histol Histopathol. 2012;27:459–66.
44. Gautheron J, Gores GJ, Rodrigues CMP. Lytic cell death in metabolic liver disease. J Hepatol. 2020;73:394–408.
45. Demuynck R, Efimova I, Naessens F, Krysko DV. Immunogenic ferroptosis and where to find it? J Immunother Cancer. 2021;9: e003430.
46. Kazankov K, Jorgensen SMD, Thomsen KL, Moller HJ, Vilstrup H, George J, et al. The role of macrophages in nonalcoholic fatty liver disease and nonalcoholic steatohepatitis. Nat Rev Gastroenterol Hepatol. 2019;16:145–59.

How to cite this article: Angendohr C, Koppe C, Herebian D, Schneider AT, Keysberg L, Singer MT, et al. The ferroptosis mediator ACSL4 fails to prevent disease progression in mouse models of MASLD. Hepatol Commun. 2025;9:e0684. https://doi.org/10.1097/HC9.0000000000000684